ELSEVIER

Journal of Photochemistry and Photobiology A: Chemistry 133 (2000) 169–176

Journal of Photochemistry and Photobiology A:Chemistry

www.elsevier.nl/locate/jphotochem

Photophysical and photochemical properties of C-linked ribosides of pyridin-2-one

G. Wenska [a], B. Skalski [a,*], Z. Gdaniec [b], R.W. Adamiak [b], J. Matulic-Adamic [c], L. Beigelman [c]

[a] *Faculty of Chemistry, A. Mickiewicz University, Poznan, Poland*
[b] *Institute of Bioorganic Chemistry, Polish Academy of Sciences, Poznan, Poland*
[c] *Department of Organic Chemistry, Ribozyme Pharmaceuticals Inc., Boulder, CO, USA*

Received 21 October 1999; received in revised form 1 February 2000; accepted 7 February 2000

Abstract

Absorption and emission properties as well as photochemical behavior of C-ribosides bearing pyridone as the aglycone, namely 5-(β-D-ribofuranosyl)-pyridin-2-one (**1**) and 3-(β-D-ribofuranosyl)-pyridin-2-one (**2**) and pyridone-uridine bichromophoric compound (**6**) have been investigated. Photocycloisomerization of the pyridone ring leading to diastereomeric Dewar type photoproducts is the major photochemical pathway both in C-nucleosides **1**,**2** and the bichromophoric compound **6**. In the case of the photocycloisomerization of **1** diastereomeric excess of 26% was determined by HPLC.

Keywords: C-nucleoside; Pyridin-2-one; Fluorescence; Photochemistry

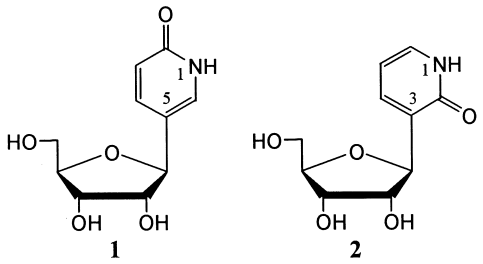

Scheme 1.

1. Introduction

It has been demonstrated lately that pyridin-2-one can serve as a nondisruptive pyrimidine analog in DNA duplex [1]. Recently, pyridin-2-one C-nucleosides **1** and **2** (Scheme 1) have been synthesized [2,3] as the modified uridine analogues that lack one of the two lactam systems NH-C(2)O and NH-C(4)O, respectively. These compounds exhibit novel H-bonding patterns and therefore can serve as valuable tools in nucleic acids structure–activity studies. Moreover, due to the presence of the pyridone chromophore they exhibit interesting spectral properties. In particular they absorb in the near UV range (λ>300 nm) where common nucleic acid bases are transparent, and exhibit room temperature fluorescence. These properties, allowing for selective excitation in an oligonucleotide chain, make these compounds interesting also as potential fluorescent and/or photochemical probes in nucleic acids. In order to evaluate those possibilities we have undertaken detailed absorption and fluorescence as well as photochemical studies of both compounds. The results of these studies are reported and discussed in this paper.

2. Experimental

2.1. Instruments

A Waters 600E HPLC equipped with Waters 991 Photodiode Array UV and Waters 470 Scanning Fluorescence detectors was used for analytical and semi-preparative scale separations. The analyses were performed using Waters radial compression Nova-Pak C-18 column segments, 8 mm×100 mm and 25 mm×100 mm for analytical and preparative runs, respectively. ^{1}H and ^{13}C NMR spectra were recorded on a Varian Unity 300 (300 MHz for ^{1}H) in D_2O with dioxane as an internal reference. All chemical shifts are converted to TMS scale (dioxane ^{1}H δ=3.71 ppm; dioxane ^{13}C δ=67.4 ppm). High resolution liquid secondary

* Corresponding author.
E-mail address: bskalski@main.amu.edu.pl (B. Skalski)

1010-6030/00/$ – see front matter
PII: S1010-6030(00)00236-7

Table 1
UV absorption and fluorescence spectral data for compounds **1** and **2** in various solvents

Component	Solvent	Absorbance		Fluorescence			
		λ_1 (ε) nm ($M^{-1}\,cm^{-1}$)	λ_2 (ε) nm ($M^{-1}\,cm^{-1}$)	λ (nm)	φ[a]	τ[b] (ns)	k_f[c] ($\times 10^7\ s^{-1}$)
1	Water pH 6	228 (9900)	297 (5000)	360	0.006	0.084	7.7
	Water pH 13	235 (12840)	295 (4040)	357	0.050	1.025	4.9
1	Methanol	229 (9960)	302 (4400)	370	0.016	0.180	8.9
1	Butanol	230 (11650)	302 (4940)	370	0.018	0.191	9.4
1	Acetonitrile	232 (10600)	305 (4510)	378	0.008	0.100	8.0
1	Dioxan	234 (11680)	306 (5040)	379	0.008	0.164	4.9
2	Water pH 6	228 (5640)	298 (6560)	365	0.043	0.330	13.1
	Water pH 13	231 (7600)	295 (5940)	357	0.087	0.835	10.5
2	Methanol	229 (5490)	299 (6410)	375	0.053	0.395	13.4
2	Butanol	230 (4760)	299 (5480)	375	0.057	0.420	13.6
2	Acetonitrile	230 (4300)	299 (5600)	377	0.025	0.190	13.2
2	Dioxan	231 (4430)	300 (5400)	380	0.030	0.223	13.4

[a] The estimated errors do not exceed 10%.
[b] The estimated errors do not exceed 5% for the lifetimes τ>200 ps, and are within the range of 5–10% for the liftimes τ<200 ps.
[c] The values of radiative rate constant k_F calculated from experimentally determined quantum yields and lifetimes using the relationship $k_F=\varphi_F/\tau_F$.

ion mass spectral analyses (HR-LSIMS) were performed on AMD Intectra Model 604 double focusing, reversed geometry instrument fitted with cesium ion gun operating at ion energy of about 12 keV and accelerating voltage 8 kV. Samples were dissolved in glycerol and analyzed in positive ion mode. UV absorption spectra were recorded on a Perkin Elmer Lambda 17 UV–VIS spectrophotometer. Steady-state fluorescence emission and excitation spectra were recorded on a Perkin Elmer LS-50B luminescence spectrophotometer. Recorded spectra were corrected for the response characteristics of the instrument. Fluorescence quantum yields were determined using quinine sulfate in 0.1 N H_2SO_4 as a standard [4]. Fluorescence decay curves were obtained by the time-correlated single photon counting (TCSPC) technique. The excitation source was the pico/femtosecond Ti:Sapphire 'Tsunami' laser pumped with a 'BeamLock' 2060 argon ion laser (Spectra-Physics).

2.2. Chemicals

All the solvents (spectrograde) used in photophysical studies were purchased from Aldrich and were used as received. The preparation of **1** and **2** (Table 1) was described previously [2,3]. 3-(ω-Bromopropyl)uridine, **5**, was obtained by alkylation of uridine with 1,3-dibromopropane in dry DMF in the presence of anhydrous potassium carbonate [5]. The crude product was purified by reversed-phase HPLC. The column was eluted isocratically with 20% aq. solution of acetonitrile (v=4 ml min^{-1}) to give analytically pure sample of **5** as an oil (70% yield). ^{1}H NMR: (CD_3OD) δ 8.04 (1H, d, J=8.1 Hz, H6-U), 5.91 (1H, d, J=3.8 Hz, H1′), 5.77 (1H, d, J=8.1 Hz, H5-U), 4.20–4.13 (2H, m, H2′, H3′), 4.07–4.00 (3H, m, H4′, $BrCH_2$), 3.86 (1H, dd, J=2.9 Hz, J=12.2 Hz, H5′), 3.74 (1H, dd, H5′′), 3.46 (2H, t, J=6.9 Hz, NCH_2), 2.17 (2H, m, J=6.9 Hz, CH_2); ^{13}C NMR (CD_3OD): δ 156.02 (C4), 143.60 (C2), 131.93 (C6), 93.00 (C5), 82.59 (C1′), 77.23 (C4′), 66.86 (C2′), 62.02 (C3′), 53.06 (C5′), 32.15 (linker), 22.97 (linker), 22.22 (linker); HRMS: calculated for $C_{12}H_{17}BrN_2O_6(M^+)$ 364.02701, found 364.02555.

Bichromophoric compound **6** was obtained by reacting of **1** (50 mg, 0.22 mmol) with **5** (80.3 mg, 0.22 mmol) in dry DMF (3 ml) in the presence of anhydrous potassium carbonate (45 mg, 0.33 mmol). As revealed by HPLC analysis of the reaction mixture (Nova-Pak C-18 column eluted with 15% aq. acetonitrile (v=0.8 ml min^{-1}), after 48 h only ca. 20% of 1 was converted into desired bichromophoric compound **6**. The crude product was subjected to preparative HPLC separation to give pure **6** (18.6 mg, 16.5% yield) as colorless oil. ^{1}H NMR: (D_2O) δ 7.84 (H6-U), 7.79 (H6-P), 7.69 (H4-P), 6.67 (H3-P), 5.91 (H5-U), 5.88 (H1′-U), 4.62 (H1′-P), 4.30 (H2′-U), 4.19 (H3′-U), 4.17 (H3′-P), 4.12 (H4′-U), 4.06 (H2′-P), 4.06, 3.96 (a,c-linker), 4.06 (H4′-P), 3.91 (H5′-U), 3.81 (H5′-P), 3.78 (H5′′-U), 3.73 (H5′′-P), 2.10 (b-linker); ^{13}C NMR: δ 165.93 (C4-U), 164.78 (C2-P), 152.53 (C2-U), 140.96 (C6-P), 140.61 (C6-U), 138.14 (C6-P), 120.47 (C5-P), 120.47 (C3-P), 102.51 (C5-U), 91.19 (C1′-U), 85.47 (C4′-P), 84.84 (C4′-U), 81.24 (C1′-P), 76.55 (C2′-P), 74.56 (C2′-U), 71.94 (C3′-P), 70.09 (C3′-U), 62.47 (C5′-P), 61.49 (C5′-U), 48.91 (linker), 39.51 (linker), 21.11 (linker); UV: (H_2O) λ_{max} (ε_{max}) 231 nm (13100), 263 nm (11020), 302 nm (5260); Fluorescence: (H_2O) λ_{max} 362 nm, φ=0.0125, τ=0.198 ns; HR-LSIMS: calculated for $C_{22}H_{30}N_3O_{11}$ (M+H) 512.18805, found 512.18876.

2.3. Photochemical experiments

Aqueous solution (100 ml) containing 1 (0.1 mM) was placed in Pyrex photoreactor, deoxygenated by bubbling with a stream of argon for 30 min and then irradiated at λ>300 nm with a high pressure mercury lamp through a Pyrex glass. The irradiation was continued until the absorption of the long wavelength absorption band (∼300 nm) decreased to 85% of its initial value. The irradiated solution

Table 2
^{1}H NMR chemical shifts δ (ppm) for photoproducts **3a**, **3b** and **4** in D_2O

Proton[a]	Photoproduct		
	3a	**3b**	**4**[b]
H-1	4.46, t, J=2.5 Hz	4.46, t, J=2.5 Hz	4.39, 4.38
H-4	4.00, m	4.01, m	–
H-5	6.50, m	6.50, m	6.54, 6.54
H-6	–	–	6.54, 6.54
H-1′	4.36, d, J=5.6 Hz	4.32, d, J=5.6 Hz	4.13, 4.05
H-2′	4.02, t, J=5.6 Hz	4.03, t, J=5.6 Hz	4.08, 3.86
H-3′	3.96, t, J=5.1 Hz	3.96, t, J=5.1 Hz	3.92, 3.88
H-4′	3.86, m	3.86, m	3.78, 3.77
H-5′	3.65, dd	3.65, dd	3.58, 3.54
H-5′′	3.53, dd	3.53, dd	3.48, 3.44

[a] For atom numbering see Scheme 2.
[b] Mixture of two diastereoisomers.

was then concentrated to a small volume and subjected to reversed phase HPLC. The C-18 column was eluted with 1% aqueous acetonitrile (v=3 ml min^{-1}). The homogeneous fractions containing photoproducts **3a** and **3b** and unreacted, starting nucleoside **1** were collected and evaporated under reduced pressure to give: **3a** (8 mg, 27.6%) and **3b** (19 mg, 65.5%) as colorless oils and **1** (5 mg) as white solid. The spectroscopic data of the photoproducts are as follows:

3a: ^{1}H and ^{13}C NMR are summarized in Tables 2 and 3, respectively; UV: (H_2O) λ 230 nm (shoulder) ε 1280 M^{-1} cm^{-1}; HR-LSIMS: calculated for $C_{10}H_{14}NO_5$ (M+H) 228.08720, found 228.08728.

3b: UV (H_2O): γ 230 nm (shoulder), ε 1310 M^{-1} cm^{-1}; HR-LSIMS: calculated for $C_{10}H_{14}NO_5$ (M+H) 228.08720, found 228.0872.

Aqueous solution of **2** (150 ml, 1 mM) was irradiated under conditions identical to those described above for **1**. The irradiation was continued until the intensity of the long wavelength absorption band dropped to ca. 34% of its initial value. The irradiated solution was concentrated under reduced pressure to a small volume and subjected to reversed-phase HPLC separation. The column was eluted with water (v=3 ml min^{-1}) to give photoproduct **4** (13 mg, 59%) and unreacted **2** (7 mg) as colorless oils. Careful analysis of the NMR spectrum of the photoproduct **4** (Table 2) revealed that it was a mixture of two diastereomers. Attempts to separate the two diastereomers by means of HPLC were unsuccessful. Therefore they were analyzed as a mixture. The respective ^{1}H and ^{13}C NMR spectral data are summarized in Tables 2 and 3, respectively; UV (H_2O) λ 230 nm (shoulder), ε 1380 M^{-1} cm^{-1}; HR-LSIMS: Calculated for $C_{10}H_{14}NO_5$ (M+H) 228.08720, found 228.08723.

Table 3
^{13}C NMR chemical shifts δ (ppm) for photoproducts **3a**, **3b** and **4** in D_2O

Carbon	Photoproduct			
	3a	**3b**	**4**[a]	
C-1	50.49	50.66	54.31	53.45
C-3	176.59	176.53	176.66	176.57
C-4	55.29	55.45	71.14	70.73
C-5	153.60	153.49	144.60	144.15
C-6	135.01	135.05	140.24	139.78
C-1′	79.68	79.60	79.47	78.61
C-2′	74.02	73.38	73.08	72.87
C-3′	72.05	72.19	72.14	71.97
C-4′	84.36	84.53	84.77	84.64
C-5′	62.60	62.56	62.60	62.48

[a] Mixture of two diastereomers.

3. Results and discussion

3.1. Spectral properties of nucleosides 1 and 2

Structures of nucleosides **1**, **2** studied in this work are presented in Scheme 1. Both compounds contain pyridone ring substituted respectively at C-5 and C-3 with the β-D-ribosyl moiety. Parent pyridone molecule has been subjected to numerous experimental and theoretical studies aimed at the understanding of its keto–enol tautomeric properties [6]. The results of these studies indicate that the keto form is a dominant species in solutions. In general, the same conclusion is reached for C-substituted pyridones, except for derivatives bearing polar substituents at C-6 position, which exist in solutions predominantly in the enol form [7–9]. Keto and enol forms of pyridone were found to exhibit distinct optical properties. In aqueous solution the keto form absorbs at λ_{max}=300 nm, whereas the enol form absorbs at λ_{max} 268 nm. Similarly in the fluorescence spectra the emission maxima of the two forms are located at 367 and 303 nm, respectively [10].

Absorption and fluorescence spectra of **1** and **2** in neutral aqueous solution are compared in Fig. 1A, whereas the relevant photophysical parameters for the two compounds in selected solvents are summarized in Table 1. As can be seen both nucleosides exhibit very similar UV spectra, except for significant difference in the ratio of the intensity of the short to long wavelength bands. In the case of **2** this ratio resembles closely that reported for 1-methylpyridone in aqueous solution [11], whereas in the case of **1**, it is much greater. Location of the long wavelength absorption band in UV spectra at ca. 300 nm in water and organic solvents indicate that similarly like the parent pyridone, **1** and **2** exist predominantly in the keto form in these solvents. The relatively high intensity of the lowest energy absorption band together with small solvent effect indicates that it originates primarily from $\pi \rightarrow \pi^*$ electronic transition.

As can be seen in Fig. 1A, the emission bands of **1** and **2** in water are well separated from respective absorption bands with the Stokes shifts amounting to ca. 6700 cm^{-1}. Similar, relatively large Stokes shifts for both compounds are also observed in other solvents used in this work. The energy of the lowest excited singlet state, calculated from the intersection of normalized absorption and fluorescence spectra, corresponds to 30,800 and 30,500 cm^{-1} for **1** and **2**, respec-

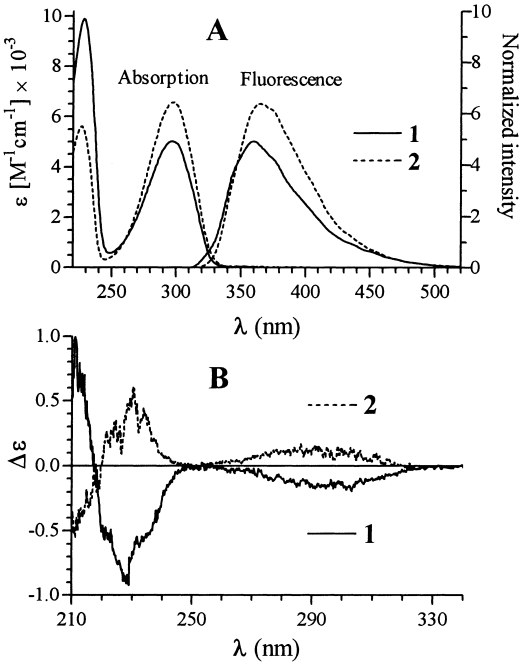

Fig. 1. UV absorption and fluorescence (A) and CD spectra (B) of **1** and **2** in water. The maxima of the fluorescence spectra were normalized to the respective long wavelength absorption maxima.

tively. These values are approximately equal to the excited singlet state energy of 2-pyridone (31,000 cm^{-1}) obtained from spectral measurements [12] and they are ca. 3000 cm^{-1} higher than that calculated for this molecule by CNDO/S method [13]. Solvent effect on the location of fluorescence maxima is more pronounced than in the case of absorption spectra. Generally, in solvents capable of forming hydrogen bonds the fluorescence maxima of **1** and **2** are slightly blue shifted, compared to those in non-H-bonding solvents of comparable polarity. This is in contrast to 2-pyridone, for which both the solvent polarity and H-bonding ability have to be accounted for rather complicated solvent effects on UV absorption and fluorescence emission spectra [12].

Comparison of the fluorescence quantum yields of **1** and **2** (Table 1) shows that **2** is more efficient fluorophore consistently in all solvents used. This is due to both the higher radiative rate constants k_F and reduced nonradiative rate constants Σk_{nr} (data not shown) in the latter. It should also be noted that the values of k_F for both compounds are relatively high and remain approximately unchanged in all the solvents used. On the other hand, these values are ca. 2–3 times lower than those calculated from the lowest energy absorption bands of **1** and **2** (250–350 nm) using Strikler Berg relation [14] ($k_F = 1.49 \times 10^8$ and 1.86×10^8 s^{-1} for **1** and **2**, respectively). These observations indicate that the emission of both compounds arises from an excited singlet state of significant π, π^* contribution and that the long wavelength absorption band may comprise, in addition to $\pi \rightarrow \pi^*$, at least one more hidden electronic transition. Indeed, theoretical calculations for parent, unsubstituted 2-pyridone predict the existence of two electronic transitions: lowest $n \rightarrow \pi^*$ at 27,500 cm^{-1} and $\pi \rightarrow \pi^*$ at 35,000 cm^{-1}, the former with very small oscillator strength [13]. In an attempt to reveal these electronic transitions, which could contribute to the lowest energy absorption band, circular dichroism spectra of compounds **1** and **2** were measured in aqueous solution (cf. Fig. 1B). As can be seen, both nucleosides exhibit very small Cotton effects, as expected for compounds in which chirality originates from the presence of dissymmetric ribosyl substituent [15]. In the spectral range of 250–350 nm only single peaks with opposite signs could be observed. In rather polar solvents used in this work the energy separation between the two states might be substantially diminished resulting in their effective mixing [16].

For both compounds the shape of fluorescence emission curves as well as the quantum yields are independent on the excitation wavelength within 250–340 nm range for each of the solvents used. Moreover, in each of the solvents, fluorescence of **1** and **2** decays monoexponentially within the subnanosecond time scale and the lifetimes are both excitation and emission wavelength independent. This indicates that in each case only one emitting species is formed upon excitation. Like in the case of parent, unsubstituted pyridone [10] no indication of phototautomerization was found, though it is frequently observed in heteroaromatic compounds containing NH–C=O system [17,18].

3.2. Effect of pH on absorption and fluorescence spectral properties of nucleosides 1 and 2

Fig. 2A shows the pH dependence of the UV absorption and fluorescence emission spectra of compound **1**. A similar set of spectra (not shown) was obtained also for compound **2**. As can be seen the UV absorption and fluorescence emission spectra of compounds **1** and **2** are insensitive to pH changes within the range of pH 4–9. For both compounds, increasing basicity of the media above pH 9.0 results in a gradual decrease in the intensity and a blue shift of the long wavelength absorption maximum with concomitant increase and a red shift of the short wavelength band (Table 1). The appearance of a single set of isosbestic points indicates that the changes in absorption spectra are due to the displacement of a single prototropic equilibrium process within the studied pH range. The ground state p*K* values of 11.40 and 11.70 for **1** and **2**, respectively, were obtained from the respective spectrophotometric tiration curves. These values are very close to that for the parent 2-pyridone, p*K*=11.63, obtained from spectrophotometric measurements [16].

As can be seen in Fig. 2B fluorescence intensity of **1** increases significantly upon going to more basic media whereas the maximum moves only slightly toward shorter wavelength (cf. Fig. 2C). Similar pH dependent spectral changes occur in the case of **2**, however, the observed increase in emission intensity is not as drastic as in the case of **1**. The spectral characteristics of anions derived from

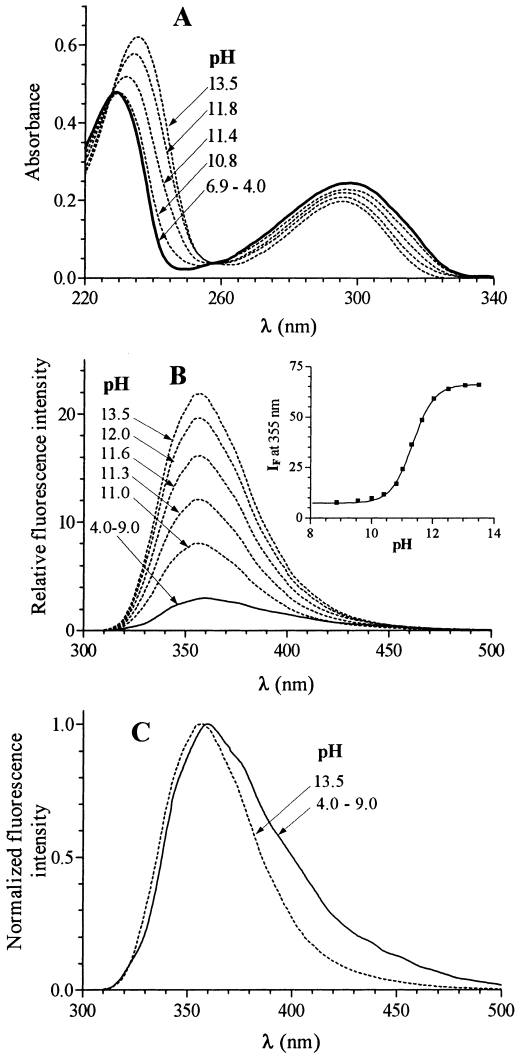

Fig. 2. The pH dependence of absorption (A) and fluorescence (B) spectra of compound **1**, inset shows the respective fluorescence titration curve. (C) Comparison of the normalized fluorescence spectra of **1** at pH 4.0–9.0 and 13.5 corresponding to protonated (neutral) and deprotonated (anionic) forms, respectively.

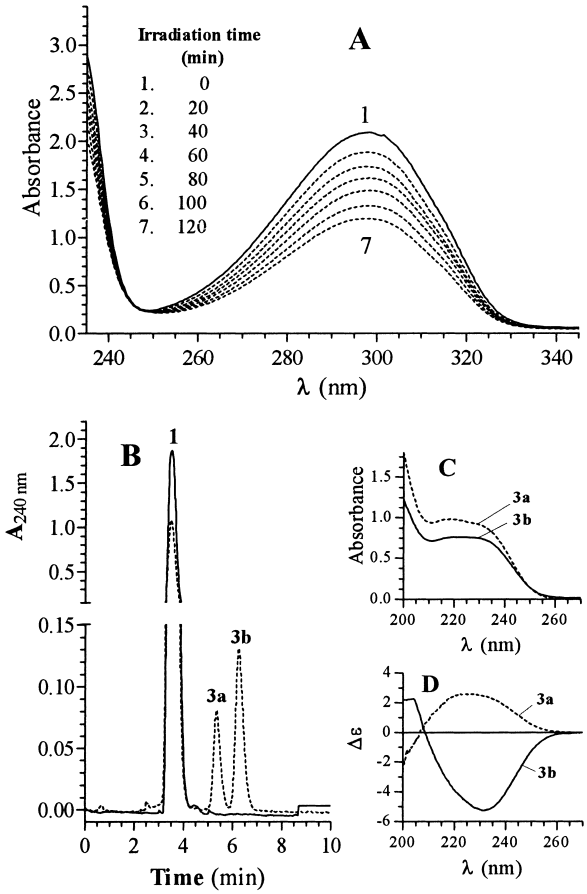

Fig. 3. (A) Changes in the absorption spectra of an aqueous solution of compound **1** during irradiation with near UV light (λ=313 nm). (B) HPLC analysis of the solution before (solid line) and after (dotted line) irradiation to ca. 50% of conversion. (C) and (D) are the UV absorption and CD spectra of the photoproducts **3a**,**b**, respectively.

both derivatives are presented in Table 1. The blue shift of λ^{F}_{max} and increase in φ_F value in basic media was reported for 2-pyridone [12,13]. The pK_a values for **1** and **2** obtained from the fluorescence titration curves (see inset in Fig. 2B) are the same as those obtained from the UV-absorption measurements indicating that pH induced fluorescence intensity changes reflect only the ground state acid-base equilibrium. Thus, no indication of excited state proton transfer reaction was found.

3.3. Photochemistry

As can be seen in Fig. 3A, irradiation of an aqueous solution of compound **1** at λ>300 nm leads to a gradual disappearance of the absorption bands at 230 and 300 nm. Concurrent HPLC analyses (Fig. 3B) of the irradiated solution revealed the conversion of **1** into two photoproducts having only end absorption at λ>220 nm (Fig. 3C). The high resolution mass spectra (see experimental) indicate that both photoproducts have the same elemental composition identical with that of the starting nucleoside **1**. Their ^{1}H and ^{13}C NMR spectral data (Section 2) are in full agreement with the diastereomeric Dewar type structures **3a**,**b** (Scheme 2) formed as a result of photochemical 4π electrocyclization of 2-pyridone residue [19–21]. The diastereomeric relationship between **3a**,**b** was confirmed further by their CD spectra which are presented in Fig. 3D. However, the available spectral data were not sufficient to establish their absolute configuration.

Irradiation of each of the photoproducts **3a**,**b** at 254 nm, restores the absorption bands characteristic for **1**, which indicates that the photoelectrocyclization of the latter is photoreversible. The sequential UV spectra recorded during the irradiation of **3a** in aqueous solution are presented in Fig. 4A. Irradiation leads to a mixture which consists of compound **1** (40.5%) and photoproduct **3a** (59.5%) as determined by HPLC (Fig. 4B). The quantum yield of the photoreversal

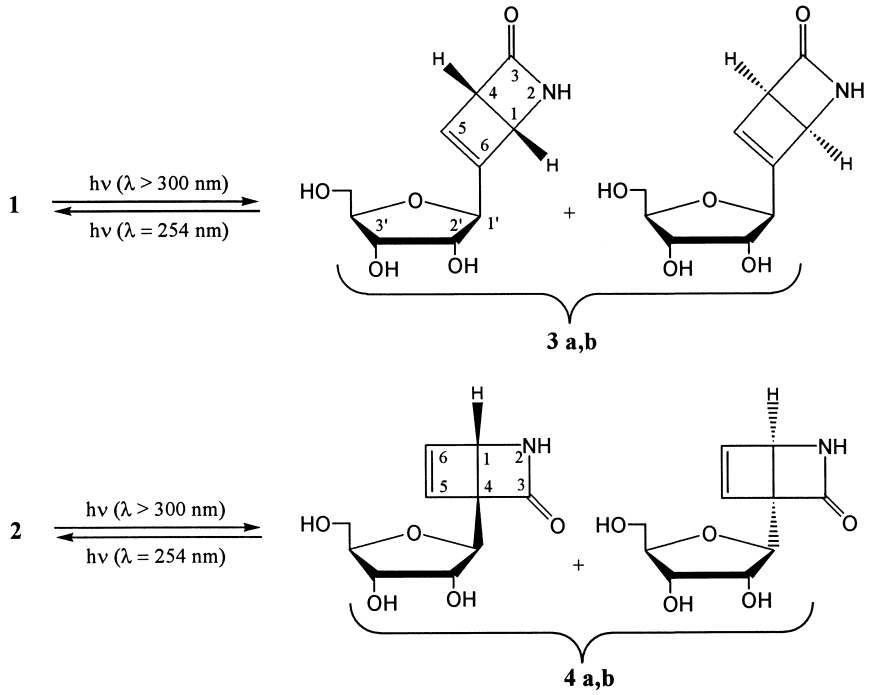

Scheme 2.

3a→**1** was found to be five times higher than that of the photocyclization **1**→**3a**. Similarly as in the case of **1**, irradiation of an aqueous solution of compound **2** under identical experimental conditions leads to the Dewar type photoproducts **4a**,**b** (Scheme 2) which, contrary to **3a**,**b**, could not be separated by chromatography and therefore were characterized as a mixture of isomers. The spectroscopic data obtained for the photoproducts **4a**,**b** (see Experimental) and their photoreversibility to compound **2** upon irradiation at 254 nm are in full agreement with the assigned structure.

The quantum yields of the photoelectrocyclization of **1** and **2** in aqueous solutions equal to 0.005 and 0.007, respectively. The presence of oxygen has no effect on both the photoproducts distribution and reaction quantum yields. Furthermore, the electrocyclization reactions of **1** and **2** do not occur under the triplet state sensitization conditions i.e. in 10% aqueous acetonitrile with benzophenone (E_T=69.2 kcal mol^{-1} [22]) as a photosensitizer (the triplet state energy for 2-pyridone was found to be 62 kcal mol^{-1} [23]). These observations indicate that formation of the Dewar type photoproducts **3a**,**b** and **4a**,**b** proceeds most likely from the excited singlet state of **1** and **2**. The involvement of an excited singlet state in the formation of Dewar type photoproducts has been reported for other 2-pyridones [24,25]. Noteworthy feature of the photoelectrocyclization of nucleosides **1** and **2** is an asymmetric induction which leads to the preferable formation of one diastereomer. In

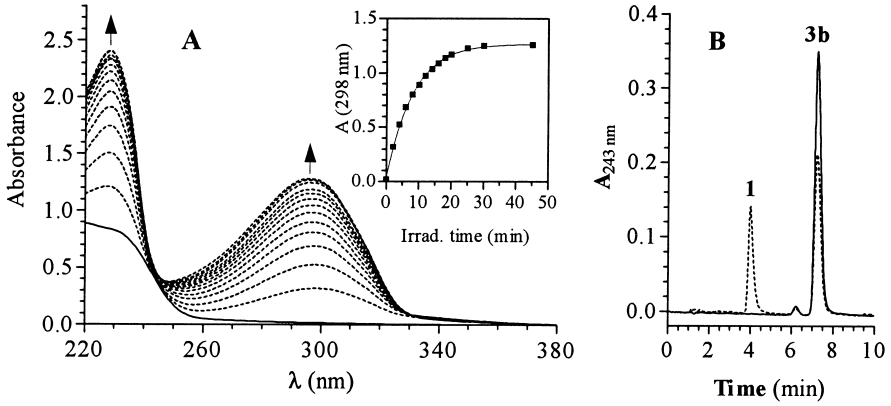

Fig. 4. (A) Changes in the UV absorption spectra of the photoproduct **3b** upon irradiation with short wavelength UV light (λ=254 nm) and the respective kinetic plot (inset). (B) HPLC analysis of the solution before (solid line) and after 40 min of irradiation (dotted line).

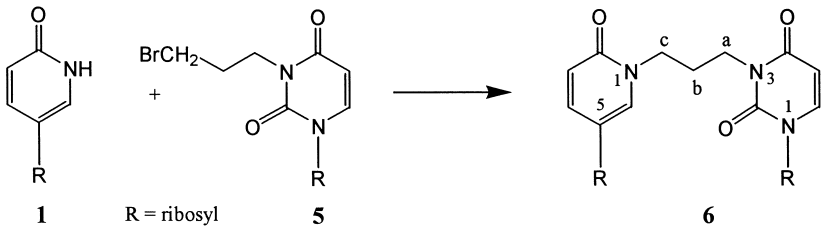

Scheme 3.

the case of **3a**,**b** the relative proportions of the two diastereomers **3a**/**3b**=1/1.7 were determined from the HPLC analysis giving rise to the diastereomeric excess of 26%. In the case of non separable mixture of the diastereomers **4a**,**b** the ^{1}H NMR spectrum analysis indicates that they are also formed in different quantities.

The 4π electrocyclization photoreaction appears to be a general reaction of 2(1H)pyridones, however, the photoproducts obtained from achiral 2-pyridones are usually racemic mixtures. The formation of optically active diastereomers of 2-β-D-ribofuranosyl-3-oxo-2-azabicyclo[2.2.0]hex-5-enes upon irradiation of 3-deazauridine was reported, but no asymmetric induction was observed [26]. Two diastereomers of Dewar pyridone were isolated from irradiation of 4-(L-methoxy)-2-pyridone with the diastereomeric excess of ca. 17% [27].

Besides the intramolecular photocycloisomerization, pyridone was shown to undergo photodimerization [28] as well as inter and intramolecular [2+2] photocycloaddition reaction with various ethylenes [23,29]. In order to test the possible photocycloaddition reaction of the pyridone with the pyrimidine residues in RNA or DNA chains a dinucleotide model compound in which the pyridone nucleoside **1** and uridine were linked by a threemethylene bridge between the 1 and 3′ positions, respectively (Scheme 3) was synthesized. Irradiation of a dinucleotide model compound **6** at λ=313 nm results in a gradual disappearance of the 300 nm absorption band (Fig. 5A) characteristic for the pyridone moiety, whereas that at 260 nm part remains practically unchanged. Concomitant HPLC analysis of the irradiated solution (Fig. 5B) reveals the formation of two photoproducts, **7a**,**b**, having identical absorption spectra with the maxima at λ=265 nm characteristic for the uridine (Fig. 5C). These observation indicate clearly, that the only reaction occurring upon selective excitation of the pyridone moiety in the bichromophoric compound **6** is the photocycloisomerization of the former leading to diastereomeric products **7a**,**b** (Scheme 4). The proposed structures of the products are in full agreement with the data obtained from mass spectrometry.

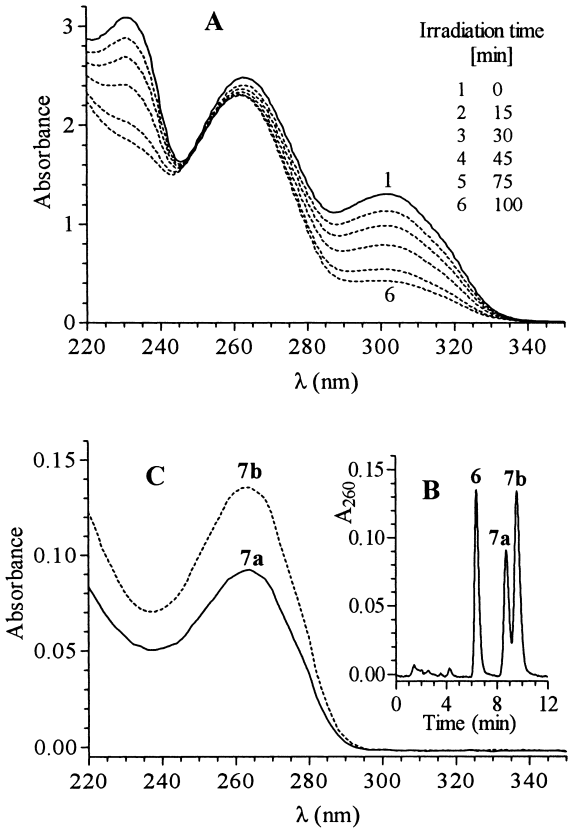

Fig. 5. (A) Time course of the spectral changes during irradiation (λ=313 nm) of an aqueous solution of the dinucleotide model compound **6**. (B) HPLC analysis of the irradiated solution. (C) The UV spectra of the photoproducts **7a**,**b**.

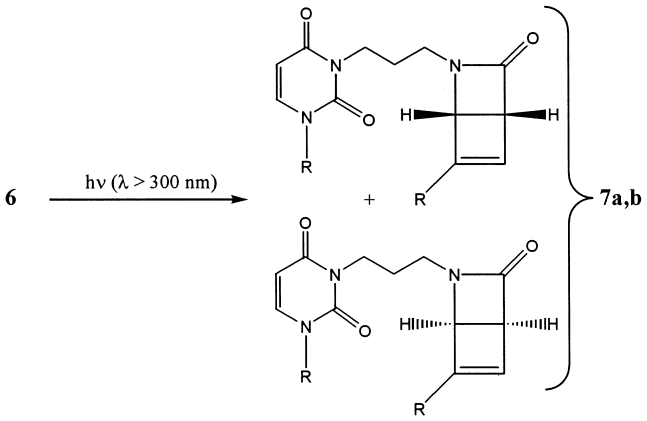

Scheme 4.

3.4. Concluding remarks

The results of the photophysical studies presented in this paper show that both solvent polarity and H-bonding capability have rather little effect on absorption and emission properties of the C-nucleosides **1** and **2**. Similarly like in the case of the parent pyridone chromophore, both in aqueous solutions within the pH range of 4–9.5 and in organic solvents the two compounds exist primarily in the neutral keto form. At pH above 9.5 they undergo deprotonation to form anionic species with the pK_a values of 11.40 and 11.70 for **1** and **2**, respectively. No phototautomerization or excited state proton transfer occurs in both nucleosides. The major photochemical process occurring upon UV irradiation of the pyridone C-nucleosides is the photocycloisomerization of the pyridone residues leading to diastereomeric Dewar type photoproducts. The observed diastereomeric excess of 26% in the case of the photocycloisomerization of **1** may have some practical meaning. As in the case of **1** and **2**, selective excitation of pyridone residue in the bichromophoric compound **6**, leads to the respective diastereomeric Dewar type photoproducts, exclusively.

Acknowledgements

Support from the State Committee for Scientific Research, The Republic of Poland is acknowledged.

References

[1] M.S. Solomon, P.B. Hopkins, J. Org. Chem. 58 (1993) 2232.
[2] J. Matulic-Adamic, L. Beigelman, Tetrahedron Lett. 38 (1997) 203.
[3] J. Matulic-Adamic, L. Beigelman, Tetrahedron Lett. 38 (1997) 1669.
[4] D.F. Eaton, Pure Appl. Chem. 60 (1998) 1107.
[5] N.J. Leonard, R.L. Cundall, J. Am. Chem. Soc. 96 (1974) 5904.
[6] A. Katritzky, C.W. Reese, E.F.V. Scriven (Eds.), Comprehensive Heterocyclic Chemistry, 2nd Edition, Pergamon, 1996, Vol. 5, p. 15.
[7] A.R. Katritzky, J.D. Rowe, S.K. Roy, J. Chem. Soc. (B) (1967) 758
[8] G. Simchen, Chem. Ber. 103 (1970) 407.
[9] E. Spinner, G.B. Yeoh, J. Chem. Soc. (B) (1971) 279.
[10] V. Barone, C. Adamo, J. Photochem. Photobiol A: Chem. 80 (1994) 211.
[11] S. F. Mason, J. Chem. Soc. (1957) 5010.
[12] A. Weisstuch, P. Neidig, A. Testa, J. Luminescence 10 (1975) 137.
[13] A. Testa, J. Photochem. Photobiol. A: Chem. 64 (1992) 73.
[14] S.J. Strikler, R.A. Berg, J. Chem. Phys. 37 (1962) 814.
[15] A. Rodger, B. Norden, Circular Dichroism and Linear Dichroism, Oxford University Press, Oxford, 1997.
[16] N.J. Turro, Modern Molecular Photochemistry, Benjamin/Cummings, Menlo Park, CA, 1978.
[17] M. Terazima, T. Azumi, J. Am. Chem. Soc. 111 (1989) 3824.
[18] J. Sepiol, H. Bulska, A. Grabowska, Chem. Phys. Lett. 140 (1987) 607.
[19] E.J. Corey, J. Streith, J. Am. Chem. Soc. 86 (1964) 950.
[20] R.C. De Selms, W.R. Schleigh, Tetrahedron Lett. 34 (1972) 3563.
[21] E. Sato, Y. Ikeda, Y. Kanaoka, Heterocycles 26 (1987) 1611.
[22] S.L. Murov, I. Carmichel, G.L. Hug, Handbook of Photochemistry, 2nd Edition, Marcel Dekker, 1993.
[23] T. Suishu, S. Tsuru, T. Shimo, K. Somekawa, J. Heterocyclic Chem. 34 (1997) 1005.
[24] H. Fuji, K. Shiba, C. Kaneko, J. Chem. Soc., Chem. Commun. (1980) 537
[25] C. Kaneko, K. Shiba, H. Fuji, Y. Momose, J. Chem. Soc., Chem. Commun. (1980) 1177.
[26] N. Katagiri, T. Haneda, C. Kaneko, Nucleic Acid Res., Symp. Series 16 (1985) 113.
[27] M. Sato, N. Katagiri, M. Muto, T. Haneda, C. Kaneko, Tetrahedron Lett. 16 (1986) 6091.
[28] Y. Nakamura, T. Kato, Y. Morita, J. Chem. Soc. Perkin I (1982) 1187.
[29] K. Somekawa, H. Okuhira, M. Sendayama, T. Suishu, T. Shimo, J. Org. Chem. 57 (1992) 5708.